Immunohistochemical Validation of PSMA Expression Measured by ^{68}Ga-PSMA PET/CT in Primary Prostate Cancer

Nadine Woythal[1], Ruza Arsenic[2], Carsten Kempkensteffen[3], Kurt Miller[4], Jan-Carlo Janssen[5], Kai Huang[1], Marcus R. Makowski[5], Winfried Brenner[1], and Vikas Prasad[1]

[1]Department of Nuclear Medicine, Charité Universitätsmedizin Berlin, Berlin, Germany; [2]Institute of Pathology, Charité Universitätsmedizin Berlin, Berlin, Germany; [3]Department of Urology, Franziskus-Krankenhaus Berlin, Berlin, Germany; [4]Department of Urology, Charité Universitätsmedizin Berlin, Berlin, Germany; and [5]Department of Radiology, Charité Universitätsmedizin Berlin, Berlin, Germany

^{68}Ga-labeled prostate-specific membrane antigen (^{68}Ga-PSMA) PET/CT has a proven role in staging and restaging of prostate cancer (PCA). The aims of this study were to evaluate the association of intraprostatic ^{68}Ga-PSMA PET/CT findings and PSMA expression in immunohistochemical staining and generate a cutoff value for differentiation between normal prostate (PN) and PCA. **Methods:** The data of 31 patients (mean age, 67.2 y) who underwent prostatectomy and preoperative PET were retrospectively analyzed. On PET, focally increased uptake in the prostate was suggestive of tumor. A region of interest was placed on the suggestive area to generate an SUV_{max}; a similar region of interest was placed on adjacent visually PN. Both PCA and PN were stained with monoclonal anti-PSMA antibody (clone 3E6, 1:100, M3620). **Results:** All intraprostatic PCA lesions on PET could be confirmed histopathologically. In PN sections ($n = 31$), median staining intensity was mild, median percentage of stained cells was 20% ± 14.24%, and median immunoreactive score (IRS) was 1. In PCA sections ($n = 31$), median IRS was 3, median staining intensity was strong, and median percentage of stained cells was 80% ± 16.46%. The mean SUV_{max} (±SD) of PCA (14.06 ± 15.56) was significantly higher than that of PN (2.43 ± 0.63; $P < 0.001$). Receiver-operating-characteristic curve analyses of the SUV_{max} of PCA, validated by immunohistochemical staining in 62 tissue samples, showed the best cutoff to be 3.15 (sensitivity, 97%; specificity, 90%; area under curve, 0.987). Applied to multifocal PCA, it resulted in sensitivity and specificity of 87% and 97% respectively. The mean SUV_{max} of PCA and PN for an IRS of less than 2 ($n = 26$; 2.52 ± 0.64) was significantly lower than the mean SUV_{max} for an IRS of 2 or more ($n = 36$; 12.38 ± 15.02; $P < 0.001$). The mean SUV_{max} was significantly lower in PCA samples with fewer than 50% stained cells ($n = 30$; 2.81 ± 2.35) than in samples with 50% or more ($n = 32$; 13.34 ± 15.55; $P < 0.001$). There was no correlation between the SUV_{max} of PCA and Gleason score ($P = 0.54$). **Conclusion:** This study showed that SUV_{max} on ^{68}Ga-PSMA PET/CT correlates significantly with PSMA expression in primary PCA, enabling the detection of PCA with a high sensitivity and specificity.

Key Words: prostate cancer; prostate specific membrane antigen; ^{68}Ga-PSMA PET/CT; immunohistochemistry; SUV_{max} cutoff

J Nucl Med 2018; 59:238–243
DOI: 10.2967/jnumed.117.195172

Prostate cancer (PCA) is the most commonly diagnosed cancer and the second leading cause of cancer death among men in the western world. The lifetime probability of being diagnosed with PCA is 14% (*1*). The usual diagnostic tools for PCA include prostate-specific antigen testing, digital rectal palpation, transrectal ultrasound, prostate biopsy, and histopathologic examination (*2–4*). Additionally, further imaging techniques such as MRI, bone scintigraphy, CT, and PET/CT are used for staging primary PCA and restaging biochemical recurrences (*2,5*). Currently, multiparametric MRI is the imaging tool recommended for detection of primary PCA and subsequent biopsy. The MRI results are evaluated on the basis of the Prostate Imaging Reporting and Data System, which grades parameters such as T2-weighted imaging, diffusion-weighted imaging, dynamic contrast-enhanced imaging, and MR spectroscopy on a 5-point scale and describes the risk of PCA, its aggressiveness, its localization, and relevant incidental findings (*6*). Diagnostic reliability appeared to be highest for tumors in the peripheral and central zones but is limited for tumors in the transitional zone (*5*). Therefore, there is a need for a more reliable imaging modality that dependably discloses all parts of the prostate gland and can be used even in patients with contraindications to MRI.

Recent studies reported that ^{68}Ga-labeled prostate-specific membrane antigen (^{68}Ga-PSMA) PET/CT has excellent detection rates for lymph node metastases, skeletal metastases, local relapses, and soft-tissue metastases compared with other PET tracers such as ^{18}F- and ^{11}C-labeled choline derivatives (*7–11*). The sensitivity and specificity for detecting local PCA using ^{11}C- and ^{18}F-choline have been reported to be 73% and 91%, respectively (*2*).

PSMA is a transmembrane protein with significantly increased expression in the cells and metastases of PCA compared with normal prostate (PN) and other physiologically PSMA-expressing tissues such as the brain, the lacrimal and salivary glands, and the proximal tubules of the kidneys (*9,10,12,13*). PSMA expression correlates with higher serum levels of prostate-specific antigen

Received Apr. 24, 2017; revision accepted Jul. 6, 2017.
For correspondence or reprints contact: Vikas Prasad, Department of Nuclear Medicine, Charité Universitätsmedizin Berlin, Charitéplatz 1 10117 Berlin, Germany.
E-mail: vikas.prasad@charite.de
Published online Aug. 3, 2017.

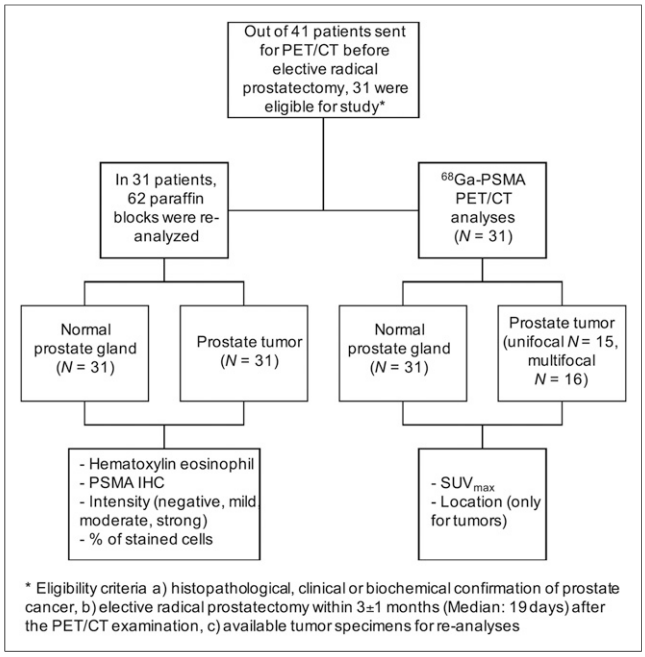

FIGURE 1. Study design.

and higher Gleason scores (GS) (*8,14*). The mean SUV_{max} of ^{68}Ga-PSMA in PN is therefore usually 4 times lower than that in PCA (*4*).

However, to our knowledge, no study has specifically evaluated whether SUV_{max} on ^{68}Ga-PSMA PET/CT correlates with PSMA expression rates and percentage of PSMA-positive cells on immunohistochemical staining. The aims of this monocentric study were to perform such an evaluation and to generate a cutoff SUV_{max} for differentiation between PN and PCA.

MATERIALS AND METHODS

Ethics, Data Search, and Patient Selection

This retrospective study was approved by the institutional ethics review board (EA4/039/17), and all subjects signed an informed consent form. To be included, the patients had to have received histopathologic, clinical, or biochemical confirmation of PCA; undergone elective radical prostatectomy within 3 mo after the PET/CT examination; and have tumor specimens available for reanalyses so that we could correlate the histopathologic findings with the imaging results. All patients who had been examined in the Department of Nuclear Medicine from May 2014 until October 2016 were selected from the ^{68}Ga-PSMA PET/CT database. Forty-one of them had undergone PET/CT because there was a high degree of suspicion of, or histopathologically confirmed, PCA. Thirty-one of these 41 patients met the inclusion criteria (Fig. 1). At first, we looked at the PET/CT images to localize the intraprostatic PCA; later, we correlated this location with the corresponding tumor specimen slides. We also compared the preoperative MRI reports with PET/CT findings.

Immunohistochemistry

Formalin-fixed, paraffin-embedded tissue sections 4 μm thick from the Institute of Pathology were reevaluated and used for subsequent immunostaining. In 31 patients, a sufficient archival tissue specimen was available for immunohistochemical staining. Routine hematoxylin- and eosin-stained sections were used for diagnosis and reevaluation. After being mounted on Superfrost Plus slides (Fisher Scientific), the paraffin sections were dewaxed and rehydrated to water by a series of graduated ethanol washes. For antigen staining, the sections were incubated for 20 min in a microwave oven (800 W) using ethylenediaminetetraacetic acid buffer (10 mmol/L; pH 8.0). Monoclonal anti-PSMA (clone 3E6, 1:100, M3620 [Dako]) was used, and the tumor sections were incubated with the antibody at room temperature for 1 h. Then, the sections were counterstained with hematoxylin and finally analyzed. The immunohistochemical results were reported as staining intensity and percentage of positively staining cells following the immunoreactive score (IRS) and modified with a 4-point IRS classification (Table 1) (*15*). The immunohistochemical analysis was performed by 2 independent investigators.

Imaging Protocol

^{68}Ga was eluted from a ^{68}Ge/^{68}Ga generator (Eckert and Ziegler Radiopharma GmbH). PSMA-HBED-CC (ABX GmbH) was labeled with ^{68}Ga. PET/CT imaging was performed 60.9 ± 26.13 min after intravenous injection of 117.23 ± 19.86 MBq (Table 2). A Gemini TF 16 PET/CT scanner (Philips) was used. The 3-dimensional acquisition mode was used for all PET scans. Axial, sagittal, and coronal slices were reconstructed (144 isotropic voxels 4 mm^3 each) using the standard reconstruction algorithm. Before the PET scan, a low-dose CT scan was obtained for anatomic mapping and attenuation correction (30 mAs, 120 kVp). Each bed position was acquired for 1.5 min, with a 50% overlap.

Image Analysis

The images were analyzed on an Extended Brilliance Workspace workstation (Philips). The scans were reread by 2 nuclear medicine clinicians with more than 10 y of experience in reporting on PET studies. Any focal prostatic uptake higher than uptake in the circumferential tissues was considered pathologic. In addition, SUV_{max} was measured in the nearest visually defined PN tissue adjacent to the primary tumor. For patients with a multifocal primary tumor, PN SUV_{max} was measured

TABLE 1
Four-Point IRS Classification

IRS	Percentage of positive cells	Intensity of staining	= IRS (0–12)
0 = negative	0 = no positive cells	0 = no color reaction	0–1 = negative
1 = mild	1 = <10% positive cells	1 = mild reaction	2–3 = mild
2 = moderate	2 = 10%–50% positive cells	2 = moderate reaction	4–8 = moderate
3 = strong	3 = 51%–80% positive cells	3 = intense reaction	9–12 = strongly positive
	4 = >80% positive cells		

Modified from Kaemmerer et al. (*15*)

TABLE 2
^{68}Ga-PSMA PET/CT Acquisition Characteristics and Findings

Characteristic	Frequency	Mean ± SD
Activity (MBq)		117.23 + 19.86
Acquisition time (min after injection)		60.9 + 26.13
Primary tumor		
Unifocal	15/31 (58.4%)	
Multifocal	16/31 (51.6%)	
Lymph node metastases		
Retroperitoneal	1/31 (3.2%)	
Pelvic	4/31 (12.9%)	
Bone metastases	1/31 (3.2%)	

adjacent to the pathologic sample used for immunohistochemistry. Multifocal tumors detected on ^{68}Ga-PSMA PET/CT were validated using pathology reports. Intraprostatic lesions were documented using the 39-sector scheme and later were correlated with the corresponding pathology findings (*16*).

Statistical Analysis

Data were analyzed using IBM SPSS Statistics 24 for Microsoft Windows. An explorative data analysis was used to calculate the mean SUV_{max} of PCA and PN and with respect to IRS (<2 and ≥2) and percentage of stained cells (<50% and ≥50%). The cutoff, sensitivity, and specificity of SUV_{max} were calculated by analyzing the receiver-operating-characteristic curve. After testing for normal distributions according to the Kolmogorov–Smirnov test, the Spearman ρ-test was used to analyze the correlation between SUV_{max} and IRS, percentage of stained cells, and GS. The Mann–Whitney *U* test was used to compare the mean SUV_{max} of PN versus PCA, of IRS < 2 versus IRS ≥ 2, and of <50% stained cells versus ≥50% stained cells. All statistical analyses were 2-sided, and *P* values of less than 0.05 were considered statistically significant.

RESULTS

Patients' Data

From the 31 patients, 31 PCA samples and 31 PN samples were investigated. A PET-corresponding tumor was found for all 31 PCA samples (Fig. 1). The mean age of the patients at the time of the PET scan was 66.57 ± 8.77 y. The indication for PET was staging in 28 patients and restaging in 3 patients. Of the 3 restaged patients, one each underwent external-beam radiation therapy, brachytherapy, and androgen deprivation therapy. In all 3 patients, ^{68}Ga-PSMA PET/CT was performed at least 3 mo after the treatments. All patients underwent radical prostatectomy after PET. None of the patients developed adverse events or clinically detectable pharmacologic side effects after injection of the ^{68}Ga-PSMA.

The mean prostate-specific antigen level was 17.49 ± 20.81 ng/mL. The GS was 7 in 29% of the patients, 8 in 35.5%, and 9 in 25.8%. Detailed information about the patients' characteristics is in Table 3. Fifteen patients had a unifocal tumor, and 16 patients had a multifocal tumor. Examples of unifocal and multifocal PCAs are shown in Figures 2 and 3, respectively. One patient (3.2%) had retroperitoneal lymph node metastases, 4 (12.9%) had pelvic lymph node metastases, and one (3.2%) had bone metastases (Table 2).

Immunohistochemistry

The mean tumor size documented in the pathology report was 29.4 ± 13.7 mm (range, 9–60 mm). In PN sections ($n = 31$), the median staining intensity was mild and the median percentage of stained cells was 20% ± 14.24%; the median IRS was 1 (range, 0–2). In PCA sections, the median IRS was 3 (range, 1–3), the median staining intensity was strong, and the median percentage of stained cells was 80% ± 16.46% (Fig. 4).

SUV

SUV_{max} and uptake time, that is, the time between injection of ^{68}Ga-PSMA and acquisition of PET images, did not correlate significantly (Spearman ρ; $P = 0.963$). The mean SUV_{max} ($n = 31$; 14.06 ± 15.56) was significantly higher in PCA than in PN ($n = 31$; 2.43 ± 0.63; $P < 0.001$) (Fig. 5).

Receiver-operating-characteristic curve analyses of the SUV_{max} of PCA, validated by immunohistochemical staining in 62 tissue samples, showed the best cutoff to be 3.15, resulting in a sensitivity of 97% and a specificity of 90% (area under the curve, 0.987) (Fig. 6). When this cutoff was applied to non–immunohistochemically validated foci in multifocal PCA, it resulted in a sensitivity of 87% and a specificity of 97% for ^{68}Ga-PSMA PET/CT.

SUV_{max} and Immunohistochemical Staining

There was no correlation between mean tumor size and SUV_{max} (Spearman ρ; $P = 0.651$). The mean SUV_{max} of PCA and PN was 2.52 ± 0.64 for IRS < 2 ($n = 26$) and 12.38 ± 15.02 for IRS ≥ 2 ($n = 36$) in (Fig. 5). There was a significant difference in SUV_{max} between IRS ≥ 2 and IRS < 2 (Mann–Whitney *U* test; $P < 0.001$). The mean SUV_{max} for fewer than 50% immunohistochemically stained cells ($n = 30$) was 2.81 ± 2.35, compared

TABLE 3
Patient Characteristics

Characteristic	Frequency (%)	Mean ± SD
Age (y)		66.57 + 8.77
Radical prostatectomy	31/31 (100)	
GS	31/31 (100)	
6	2/31 (6.5)	
7	9/31 (29.0)	
8	11/31 (35.5)	
9	8/31 (25.8)	
10	1/31 (3.2)	
Prostate-specific antigen (ng/mL)	30/31 (96.8)	17.49 + 20.81
<2	0/30 (0)	
2–20	23/30 (76.7)	
>20	7/30 (23.3)	
Hormone therapy	1/31 (3.2)	
Indications		
Staging	28/31 (90.3)	
Restaging	3/31 (9.7)	

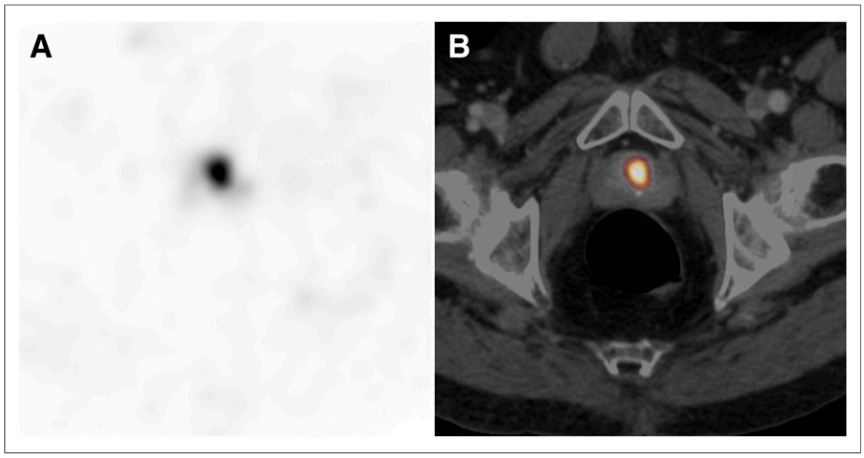

FIGURE 2. ^{68}Ga-PSMA PET/CT images showing unifocal PCA with GS of 3 + 4 = 7. (A) Axial PET image. (B) Fused PET/CT image. SUV_{max} of tumor was 13.9, IRS was 2, and 80% of cells were stained.

with 13.34 ± 15.55 for 50% or more ($n = 32$; $P < 0.001$) (Fig. 5). There was a significant difference in mean SUV_{max} between tumor specimens with more than 50% stained cells and fewer than 50% (Mann–Whitney U test; $P < 0.001$). The Spearman ρ test revealed a significant correlation between SUV_{max} and IRS ($P < 0.001$), as well as between SUV_{max} and percentage of stained cells ($P < 0.001$). The data are summarized in Table 4. The mean SUV_{max} was lower in patients with a GS of less than or equal to 8 (5.81 ± 4.7) than in patients with a GS of more than 8 (9.59 ± 14.9); however, there was no statistical correlation between SUV_{max} and GS ($P = 0.54$).

PET/CT and MRI

Of the 31 patients, 20 had preoperative MRI reports that could be retrieved from the hospital's database. The median interval between PET/CT and MRI was 2 mo. Twenty primary PCAs were seen on both PET/CT and MRI. PET/CT and MRI showed concordant results for 12 (60%) of the 20 and discordant results in the other 8 (40%). Of the 8 patients in the discordant group, PET/CT showed multifocal PCA in 7 (87.5%) whereas MRI showed unifocal disease. In the 8th patient, MRI showed multifocal intraprostatic lesions whereas PET/CT showed unifocal disease. Furthermore, PET/CT showed 6 lymph node metastases and MRI showed none.

DISCUSSION

To the best of our knowledge, this was the first study to generate a cutoff SUV_{max}, validated by immunohistochemistry, for separating PCA from PN by ^{68}Ga-PSMA PET/CT images acquired on a Gemini TF 16 scanner. This validated cutoff of 3.15 for SUV_{max} enables the diagnosis of PCA with a high sensitivity and specificity in both unifocal and multifocal disease. In a previous study by our group, an SUV_{max} of 3.2 based purely on imaging, without histopathologic confirmation, resulted in a sensitivity of 94.3% and a specificity of 100% for differentiation between PCA and PN (*4*). Retrospectively, these findings are completely in line with our new and immunohistochemically validated SUV_{max} cutoff.

Furthermore, Rahbar et al. documented a significant difference ($P < 0.001$) in median SUV_{max} between PCA (11.0 ± 7.8) and PN (2.7 ± 0.9). This result is similar to our result of 14.06 ± 15.56 and 2.43 ± 0.63 in PCA and PN, respectively (*17*). This high and specific tumor uptake occurs because PSMA, a folate hydrolase 1 or glutamate carboxypeptidase 2, is highly expressed in primary PCA and metastatic lesions (*13,18,19*). In our study, immunohistochemical

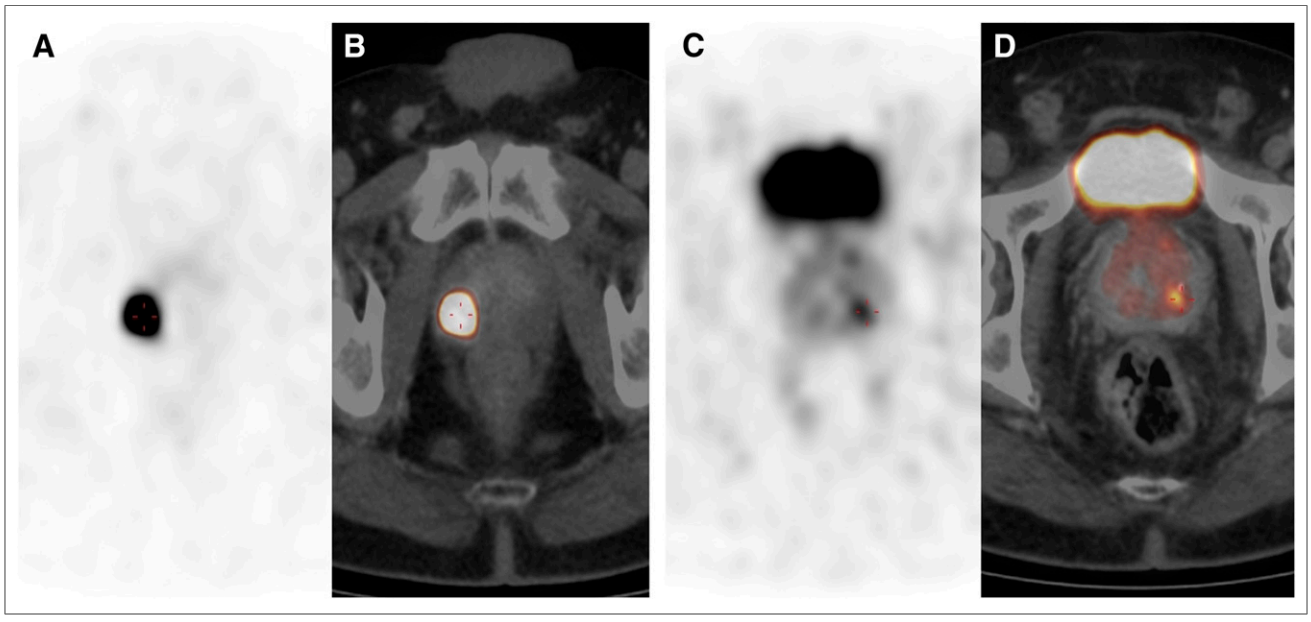

FIGURE 3. ^{68}Ga-PSMA PET/CT images showing multifocal PCA in peripheral zone with GS of 5 + 5 = 10. (A and C) Axial PET images. (B and D) Fused PET/CT images. SUV_{max} of lesion in B was 84.3 and that of lesion in D was 5.7. IRS was 3, and 80% of cells were stained.

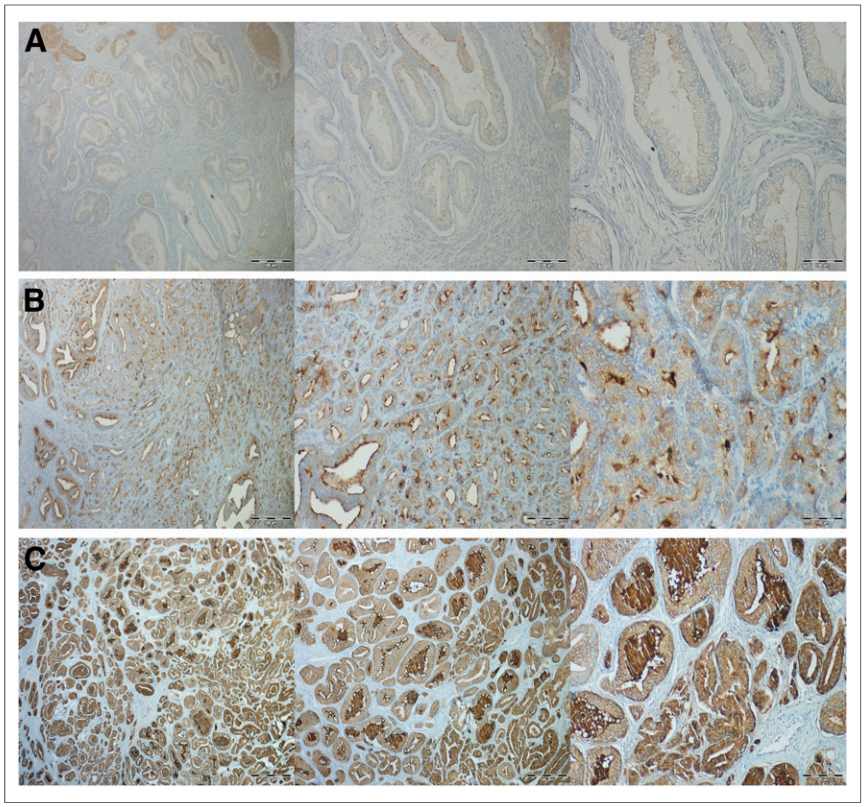

FIGURE 4. Examples of immunohistochemical staining of PNs and PCAs with IRSs of 2 and 3. Immunohistochemical staining was performed with monoclonal anti-PSMA (clone 3E6, 1:100, M3620). (A) PN (4 × 10, 10 × 10, 30 × 10). (B) IRS of 2 (4 × 10, 10 × 10, 30 × 10). (C) IRS of 3 (2 × 10, 4 × 10, 10 × 10).

PSMA staining was also more intense in PCA than in PN, confirming recent studies showing either weak or even absent immunoreactive staining in PN and hyperplastic prostate glands (*7,12,20*). Consequently, PSMA is a good target, and ^{68}Ga-PSMA PET/CT thus yields images with a high target-to-nontarget ratio. This result is of special interest in the fast-emerging field of multimodal image–guided biopsy.

Transrectal ultrasound–guided biopsy, one of the standard clinical procedures, misses a significant number of PCAs in the ventral segment of the prostate gland and in extreme lateral positions in the peripheral zone and apex. Recent studies showed that transrectal ultrasound biopsy misses around 30%–45% of PCAs in these areas (*21–23*). In patients who have undergone multiple transrectal ultrasound–guided biopsies with negative results, MRI-guided biopsy achieved detection rates of 41%–59% (*24–27*). To circumvent the problem with transrectal ultrasound, multiparametric MRI has been proposed as an adjunct alternative. Primarily performed on patients with a precedent negative biopsy result, multiparametric MRI is used to localize the primary tumor, stage the disease, plan nerve-preserving radical prostatectomy, and monitor active surveillance. In experienced centers, multiparametric MRI–generated Prostate Imaging Reporting and Data System results reach sensitivities of 85%–90% and specificities of 62%–68% (*28*). Recent reviews on the performance of Prostate Imaging Reporting and Data System versions 1 and 2 have found a high discriminative ability for tumor detection (area under the curve, 0.96 in version 1 vs. 0.90 in version 2). In comparison, the area under the curve for PET in our study was 0.987 (*29,30*). This result could have been caused by some of the limitations of multiparametric MRI mentioned previously (*28*). Among them, one clinically relevant limitation is the low detection rate in small tumors and those with a GS of less than 7 (*17*).

In our current PET study, the SUV_{max} of PCA lesions was higher when the GS was over 8 than when it was lower or equal to; however, GS did not correlate with SUV_{max} ($P = 0.54$), as was recently also shown by Ceci et al. (*9*). In a recent paper by our group, GS tended to correlate with SUV_{max} in 60 tumor lesions ($P = 0.071$) (*4*). These findings are supported by histopathologic studies in which PSMA expression was usually shown to be higher in lesions with a higher GS (*14*). Future multicenter studies with larger patient populations will finally help define the exact correlation between GS and SUV_{max} in PCA.

Irrespective of a potential correlation between SUV_{max} and GS, the uniquely high target-to-nontarget ratio as represented by a high SUV_{max} and the specific binding of the PET tracer to PSMA, in combination with the 3-dimensional PET images, should bolster the

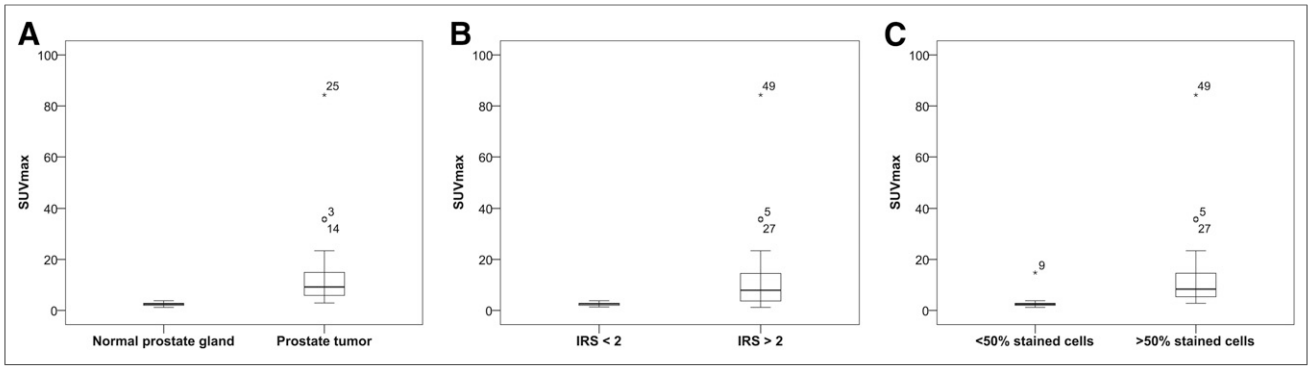

FIGURE 5. Box plots of PNs in comparison to PCAs. (A) Mean SUV_{max} was 2.43 ± 0.63 in PNs ($n = 31$) and 14.06 ± 15.56 in PCAs ($n = 31$; $P < 0.001$). (B) Mean SUV_{max} was 2.52 ± 0.64 for IRS < 2 ($n = 26$) and 12.38 ± 15.02 for IRS ≥ 2 ($n = 36$; $P < 0.001$). (C) Mean SUV_{max} was 2.81 ± 2.35 for < 50% stained cells ($n = 30$) and 13.34 ± 15.55 for ≥ 50% stained cells ($n = 32$; $P < 0.001$).

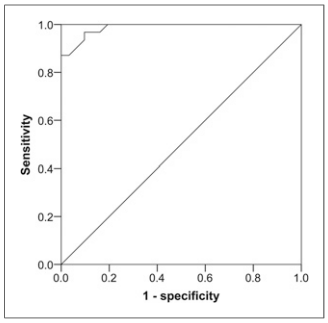

FIGURE 6. Receiver-operating-curve analysis. Cutoff of 3.15 for SUV_{max} yielded sensitivity of 97% and specificity of 90% (area under curve, 0.987).

concept of multimodal imaging and image-guided biopsy and stereotactic therapy. The retrospective data on MRI versus PET/CT of our study showed that PET information and MRI information are complementary in some patients. In this context, the combination of multiparametric MRI and ^{68}Ga-PSMA PET, ideally performed within a single examination by ^{68}Ga-PSMA PET/MRI, might become the future gold standard for localization and staging of PCA.

TABLE 4
SUV_{max} vs. Immunohistochemistry

Parameter	Mean ± SD	*P*
IRS < 2	2.52 ± 0.64	<0.001
IRS > 2	12.38 ± 15.02	
<50% stained cells	2.81 ± 2.35	<0.001
>50% stained cells	13.34 ± 15.55	

The retrospective and single-center design of our study bears a risk of biased results: a prospective multicenter study validating the clinical value of ^{68}Ga-PSMA PET/CT or even ^{68}Ga-PSMA PET/MRI in primary PCA should be performed in the future. Another limitation was the low number of patients. Finally, although the possibility of PSMA-negative PCA, potentially resulting in some false-negative ^{68}Ga PSMA PET findings, is uncommon, it cannot be excluded (*13,19*).

CONCLUSION

This study showed that SUV_{max} on ^{68}Ga-PSMA PET/CT correlates significantly with PSMA expression on primary PCA and can be used to detect and localize PCA with a high sensitivity and specificity.

DISCLOSURE

No potential conflict of interest relevant to this article was reported.

REFERENCES

1. Siegel RL, Miller KD, Jemal A. Cancer statistics, 2016. *CA Cancer J Clin.* 2016;66:7–30.
2. Schwarzenböck S, Souvatzoglou M, Krause BJ. Choline PET and PET/CT in primary diagnosis and staging of prostate cancer. *Theranostics.* 2012;2:318–330.
3. Smith RA, Andrews K, Brooks D, et al. Cancer screening in the United States, 2016: a review of current American Cancer Society guidelines and current issues in cancer screening. *CA Cancer J Clin.* 2016;66:96–114.
4. Prasad V, Steffen IG, Diederichs G, Makowski MR, Wust P, Brenner W. Biodistribution of ^{68}Ga-PSMA-HBED-CC in patients with prostate cancer: characterization of uptake in normal organs and tumour lesions. *Mol Imaging Biol.* 2016;18:428–436.
5. Röthke MC, Afshar-Oromieh A, Schlemmer HP. Potential of PET/MRI for diagnosis of prostate cancer. *Radiologe.* 2013;53:676–681.
6. Barentsz JO, Richenberg J, Clements R, et al. ESUR prostate MR guidelines 2012. *Eur Radiol.* 2012;22:746–757.
7. Budäus L, Leyh-Bannurah SR, Salomon G, et al. Initial experience of ^{68}Ga-PSMA PET/CT imaging in high-risk prostate cancer patients prior to radical prostatectomy. *Eur Urol.* 2016;69:393–396.
8. Eiber M, Maurer T, Souvatzoglou M, et al. Evaluation of hybrid ^{68}Ga-PSMA ligand PET/CT in 248 patients with biochemical recurrence after radical prostatectomy. *J Nucl Med.* 2015;56:668–674.
9. Ceci F, Uprimny C, Nilica B, et al. ^{68}Ga-PSMA PET/CT for restaging recurrent prostate cancer: which factors are associated with PET/CT detection rate? *Eur J Nucl Med Mol Imaging.* 2015;42:1284–1294.
10. Afshar-Oromieh A, Malcher A, Eder M, et al. PET imaging with a ^{68}Ga-labelled PSMA ligand for the diagnosis of prostate cancer: biodistribution in humans and first evaluation of tumour lesions. *Eur J Nucl Med Mol Imaging.* 2013;40:486–495.
11. Afshar-Oromieh A, Zechmann CM, Malcher A, et al. Comparison of PET imaging with a ^{68}Ga-labelled PSMA ligand and ^{18}F-choline-based PET/CT for the diagnosis of recurrent prostate cancer. *Eur J Nucl Med Mol Imaging.* 2014;41:11–20.
12. Silver DA, Pellicer I, Fair WR, Heston WD, Cordon-Cardo C. Prostate-specific membrane antigen expression in normal and malignant human tissues. *Clin Cancer Res.* 1997;3:81–85.
13. Mannweiler S, Amersdorfer P, Trajanoski S, Terrett JA, King D, Mehes G. Heterogeneity of prostate-specific membrane antigen (PSMA) expression in prostate carcinoma with distant metastasis. *Pathol Oncol Res.* 2009;15:167–172.
14. Ross JS, Sheehan CE, Fisher HA, et al. Correlation of primary tumor prostate-specific membrane antigen expression with disease recurrence in prostate cancer. *Clin Cancer Res.* 2003;9:6357–6362.
15. Kaemmerer D, Peter L, Lupp A, et al. Molecular imaging with ^{68}Ga-SSTR PET/CT and correlation to immunohistochemistry of somatostatin receptors in neuroendocrine tumours. *Eur J Nucl Med Mol Imaging.* 2011;38:1659–1668.
16. Weinreb JC, Barentsz JO, Choyke PL, et al. PI-RADS prostate imaging: reporting and data system—2015, version 2. *Eur Urol.* 2016;69:16–40.
17. Rahbar K, Weckesser M, Huss S, et al. Correlation of intraprostatic tumor extent with ^{68}Ga-PSMA distribution in patients with prostate cancer. *J Nucl Med.* 2016;57:563–567.
18. Yao V, Berkman CE, Choi JK, O'Keefe DS, Bacich DJ. Expression of prostate-specific membrane antigen (PSMA), increases cell folate uptake and proliferation and suggests a novel role for PSMA in the uptake of the non-polyglutamated folate, folic acid. *Prostate.* 2010;70:305–316.
19. Bostwick DG, Pacelli A, Blute M, Roche P, Murphy GP. Prostate specific membrane antigen expression in prostatic intraepithelial neoplasia and adenocarcinoma: a study of 184 cases. *Cancer.* 1998;82:2256–2261.
20. Lapidus RG, Tiffany CW, Isaacs JT, Slusher BS. Prostate-specific membrane antigen (PSMA) enzyme activity is elevated in prostate cancer cells. *Prostate.* 2000;45:350–354.
21. Lecornet E, Ahmed HU, Hu Y, et al. The accuracy of different biopsy strategies for the detection of clinically important prostate cancer: a computer simulation. *J Urol.* 2012;188:974–980.
22. Scott S, Samaratunga H, Chabert C, Breckenridge M, Gianduzzo T. Is transperineal prostate biopsy more accurate than transrectal biopsy in determining final Gleason score and clinical risk category? A comparative analysis. *BJU Int.* 2015;116(suppl 3):26–30.
23. Scattoni V, Zlotta A, Montironi R, Schulman C, Rigatti P, Montorsi F. Extended and saturation prostatic biopsy in the diagnosis and characterisation of prostate cancer: a critical analysis of the literature. *Eur Urol.* 2007;52:1309–1322.
24. Durmuş T, Reichelt U, Huppertz A, Hamm B, Beyersdorff D, Franiel T. MRI-guided biopsy of the prostate: correlation between the cancer detection rate and the number of previous negative TRUS biopsies. *Diagn Interv Radiol.* 2013;19:411–417.
25. Hambrock T, Somford DM, Hoeks C, et al. Magnetic resonance imaging guided prostate biopsy in men with repeat negative biopsies and increased prostate specific antigen. *J Urol.* 2010;183:520–527.
26. Hoeks CM, Schouten MG, Bomers JG, et al. Three-Tesla magnetic resonance-guided prostate biopsy in men with increased prostate-specific antigen and repeated, negative, random, systematic, transrectal ultrasound biopsies: detection of clinically significant prostate cancers. *Eur Urol.* 2012;62:902–909.
27. Roethke M, Anastasiadis AG, Lichy M, et al. MRI-guided prostate biopsy detects clinically significant cancer: analysis of a cohort of 100 patients after previous negative TRUS biopsy. *World J Urol.* 2012;30:213–218.
28. Junker D, Schafer G, Edlinger M, et al. Evaluation of the PI-RADS scoring system for classifying mpMRI findings in men with suspicion of prostate cancer. *Biomed Res Int.* 2013;2013:252939.
29. Haas M, Gunzel K, Penzkofer T, et al. Implications of PI-RADS version 1 and updated version 2 on the scoring of prostatic lesions in multiparametric MRI. *Aktuelle Urol.* 2016;47:383–387.
30. Auer T, Edlinger M, Bektic J, et al. Performance of PI-RADS version 1 versus version 2 regarding the relation with histopathological results. *World J Urol.* 2017;35:687–693.